EBioMedicine 39 (2019) 448–460

Contents lists available at ScienceDirect

EBioMedicine

journal homepage: www.ebiomedicine.com

EBioMedicine
Published by THE LANCET

Research paper

The partial inhibition of hypothalamic IRX3 exacerbates obesity

Thiago Matos de Araujo [a,c], Daniela S. Razolli [a], Felipe Correa-da-Silva [a], Jose C. de Lima-Junior [a], Rodrigo S. Gaspar [a], Davi Sidarta-Oliveira [a], Sheila C. Victorio [a], Jose Donato Jr [b], Young-Bum Kim [c], Licio A. Velloso [a,*]

[a] Laboratory of Cell Signaling, Obesity and Comorbidities Research Center, State University of Campinas (UNICAMP), Brazil
[b] Department of Physiology and Biophysics, Institute of Biomedical Sciences, University of São Paulo, São Paulo, SP, Brazil
[c] Divison of Endocrinology, Diabetes and Metabolism, Department of Medicine, Beth Israel Deaconess Medical Center and Harvard Medical School, Boston, MA, USA

ARTICLE INFO

Article history:
Received 10 October 2018
Received in revised form 21 November 2018
Accepted 22 November 2018
Available online 3 December 2018

ABSTRACT

Background: The *Iroquois homeobox 3* (*Irx3*) gene has been identified as a functional long-range target of obesity-associated variants within the *fat mass and obesity-associated protein* (*FTO*) gene. It is highly expressed in the hypothalamus, and both whole-body knockout and hypothalamic restricted abrogation of its expression results in a lean phenotype, which is mostly explained by the resulting increased energy expenditure in the brown adipose tissue. Because of its potential implication in the pathogenesis of obesity, we evaluated the hypothalamic cell distribution of Irx3 and the outcomes of inhibiting its expression in a rodent model of diet-induced obesity.

Methods: Bioinformatics tools were used to evaluate the correlations between hypothalamic Irx3 and neurotransmitters, markers of thermogenesis and obesity related phenotypes. Droplet-sequencing analysis in >20,000 hypothalamic cells was used to explore the types of hypothalamic cells expressing Irx3. Lentivirus was used to inhibit hypothalamic Irx3 and the resulting phenotype was studied.

Findings: IRX3 is expressed predominantly in POMC neurons. Its expression is inhibited during prolonged fasting, as well as when mice are fed a high-fat diet. The partial inhibition of hypothalamic Irx3 using a lentivirus resulted in increased diet-induced body mass gain and adiposity due to increased caloric intake and reduced energy expenditure.

Interpretation: Contrary to the results obtained when lean mice are submitted to complete inhibition of Irx3, partial inhibition of hypothalamic Irx3 in obese mice causes an exacerbation of the obese phenotype. These data suggest that at least some of the Irx3 functions in the hypothalamus are regulated according to a hormetic pattern, and modulation of its expression can be a novel approach to modifying the body's energy-handling regulation.

Fund: Sao Paulo Research Foundation grants 2013/07607-8 (LAV) and 2017/02983-2 (JDJ); NIH grants R01DK083567 (YBK).

1. Introduction

Common genetic intronic variants of the *fat mass and obesity-associated gene* (*FTO*) were identified in three independent studies as being highly associated with the obese phenotype in the general population [18,20,31]. At first, there were neither clues about the links between *FTO* intronic variants and changes in FTO function, nor evidence of the mechanisms by which humans carrying these variants would develop abnormal body adiposity [37].

In 2014, Smemo and coworkers showed that *Iroquois homeobox 3* (*Irx3*) null mice were leaner than the controls due to a hypothalamic-dependent increase in sympathetic tonus that stimulated brown adipose tissue (BAT) activity and increased energy expenditure [33]. The *Irx3* gene is located within the Ft region, half of a megabase downstream from the *Fto* gene [28]. Its promoter is regulated by long-range enhancers from the *Fto* intronic regions, providing the first evidence for a connection between *Fto* and obesity through the regulation of *Irx3* [33].

Specific subpopulations of hypothalamic neurons play central roles in the control of body adiposity by regulating caloric intake and energy expenditure [5,29,39]. Human and experimental data show that in obesity, hypothalamic neurons are affected at the functional and structural levels by an inflammatory response, triggered by the excessive consumption of dietary fats ([17,23,26,27,34,35]; van de Sande-Lee et al.,

* Corresponding author at: Laboratory of Cell Signaling, Obesity and Comorbidities Research Center, State University of Campinas (UNICAMP), 13084-970 Campinas, SP, Brazil.
E-mail address: lavelloso@fcm.unicamp.br (L.A. Velloso).

https://doi.org/10.1016/j.ebiom.2018.11.048

Research in context

Evidence before this study

The *fat mass and obesity-associated protein* (*FTO*) gene has been identified in a number of genome-wide association studies as one of the most important genes linked to human obesity. However, until recently, its actual role in obesity was unknown. In 2014, the hypothalamic expression of *Iroquois homeobox 3* (*Irx3*) gene was shown to regulate energy expenditure through the control of sympathetic outflow to the brown adipose tissue. It was also demonstrated that Irx3 promoter is regulated by long-range enhancers from the *Fto* intronic regions, providing the first evidence for a functional connection between *Fto* and obesity.

Added value of this study

Using single-cell RNA sequencing we demonstrate that hypothalamic Irx3 is almost exclusively expressed in POMC neurons. In addition, we show that partial inhibition of hypothalamic Irx3 in adult mice exacerbates the obese phenotype induced by a high-fat diet. The mechanism underlying the worsening of the obese phenotype is dependent on the reduction of brown adipose tissue thermogenic activity.

Implications of all the available evidence

POMC neurons are regarded as important potential targets for the treatment of obesity. The identification of proteins that are expressed in POMC neurons and play important roles in the control of whole body energy homeostasis may offer new opportunity for the development of optimal strategies to treat obesity. In the hypothalamus, Irx3 is almost exclusively present in POMC neurons and controls brown adipose tissue function; thus, Irx3 emerges as a potential target for the treatment of obesity.

[38,42]). One of the consequences of this abnormal hypothalamic neuronal function is a reduction of whole body energy expenditure, at least in part due to the defective regulation of BAT thermogenesis [6,30,32]. There are no previous studies investigating whether *Irx3* expression is affected in diet-induced obesity, and if so, what the consequences are of this abnormal regulation.

Here we show that hypothalamic *Irx3* is down-regulated by prolonged fasting and also by the consumption of a high-fat diet (HFD). The hypothalamic inhibition of *Irx3* results in increased body mass gain due to increased caloric intake and reduced energy expenditure, which is accompanied by reduced BAT thermogenesis. Thus, *Irx3* is abnormally regulated in diet-induced obesity, and further reducing its hypothalamic levels results in increased body mass gain.

2. Materials and methods

2.1. Animal models

Eight-week old male C57BL/6 J mice were employed in most of the experiments, except for in some of the immunofluorescence determinations, as described at the bottom of this paragraph. Mice were housed individually; temperature was controlled (22 ± 1 °C), and a 12-hour light–dark cycle was maintained. Food and water were available ad libitum throughout the experimental period, except for during some experiments designed to evaluate the effects of fasting and refeeding on IRX3 expression, as detailed under study design. In order to determine the expression of IRX3 in POMC and AgRP neurons in the hypothalamus, AgRP-Ires-Cre mice (Agrp$^{tm1(cre)Lowl/J}$, Jackson Laboratories) or POMC-Cre mice (Tg(Pomc1-cre)16Lowl/J, Jackson Laboratories) were crossed with Cre-inducible GFP-reporter mice (The Jackson Laboratory) resulting in GFP expression specifically in AgRP or POMC neurons, respectively. In addition, in another set of experiments aimed at detecting IRX3 in POMC neurons in the solitary tract nucleus (NTS), POMC-Cre mice (Tg$^{(Pomc1-cre)16Lowl}$/J, Jackson Laboratories) were crossed with the Cre-inducible GFP-reporter mouse (B6.129(Cg)-Tg(CAG-Bgeo/GFP) 21Lbe/J, The Jackson Laboratory). The mutations were confirmed by genotyping (GoTaq® G2 Green Master Mix, Promega). All experiments were performed in accordance with the guidelines of the Brazilian College for Animal Experimentation and approved by the Institutional Animal Care and Use Committee (CEUA 3549-1).

2.2. Study design

For experiments involving the HFD, mice were randomly divided into four groups and fed a HFD (55% calories from predominantly saturated fat) for one day, three days, four weeks or eight weeks. The composition of diets is presented in Supplementary Table 1. Each group was paired with a control group that was fed exclusively standard chow. For the fasting experiment mice were fed standard chow or HFD for three days, then fasted for 0, 3, 6 or 24 h. For knockdown experiments, mice underwent stereotaxic surgery for a bilateral injection of lentiviral shRNA scramble or IRX3 particles, then fed a HFD for four weeks.

2.3. Cell culture

The neuronal cell line mHypoA 2/29 CLU189 (CLU189) and the microglial cell line BV2 were cultivated to 70% confluence in Dulbecco's modified Eagle's medium (DMEM) containing 25 mM glucose and 10% fetal bovine serum. cDNAs from both cell lines were used to analyze the *Irx3* gene expression by quantitative polymerase chain reaction (qPCR).

2.4. Stereotaxic surgery

Commercially available (Sigma-Aldrich, St Louis, MO, USA) shRNA–lentiviral clones to IRX3 TRCN 0000096101 (LV1), TRCN 0000096100 (LV2), TRCN 0000096099 (LV3), TRCN 00000423725 (LV4), TRCN 00000435053 (LV5) or scramble (SHC 016 V, pLKO.1-puro non-mammalian shRNA control) (SCR) were used for knockdown experiments. Mice were anesthetized with ketamine (100 mg/kg) and xylazine (10 mg/kg) and submitted to stereotaxic surgery (Ultra Precise–model 963, Kopf). Lentiviral shRNA particles (10^6 TU) were injected bilaterally (1 μL/min) into the arcuate nucleus (ARC) (coordinates [antero-posterior/lateral/depth to bregma]: 1.7/± 0.3/−5.6 mm). The injection of Evan blue and dissection of the region of interest provided the anatomical control of stereotaxic procedure (Suppl. Fig. 1).

2.5. Indirect calorimetry and locomotor activity

Oxygen consumption (VO_2), carbon dioxide production (VCO_2), the respiratory exchange ratio (RER), energy expenditure, and total locomotor activity were measured using an indirect open-circuit calorimeter (LE405 gas analyzer, Panlab/Harvard apparatus, Holliston, MA, USA). Mice were allowed to adapt for 24 h before data were recorded for 24 h (light and dark cycles). The feeding efficiency was calculated as a ratio between total body mass gain (g) and cumulative energy intake (kcal) over 14 days, beginning after the stereotaxic surgery.

2.6. Heart perfusion and hypothalamic immunostaining

Mice were anesthetized with ketamine and xylazine, as previously described, and perfused with an intracardiac infusion of 0.9% saline,

followed by 4% formaldehyde. The brain was removed from each rodent, post-fixed for 24 h in 4% paraformaldehyde (PFA) solution, and dehydrated in a buffer containing 20% sucrose at 4 °C. A series of 30 μm-thick frozen sections were prepared using a cryostat and stored in an anti-freezing solution. For the immunostaining, slices were washed twice with 0.1 M phosphate-buffered saline (PBS), then incubated in 0.25% Triton X-100 and 5% bovine serum albumin (BSA) in 0.1 M PBS for 2 h at room temperature to block and permeablize. Slices were incubated overnight at 4 °C with primary antibodies in a blocking solution. After washing, sections were incubated with fluorophore-labeled secondary antibodies in a blocking solution for 2 h at room temperature. The antibodies used are listed in Supplementary Table 2. Nuclei were labeled with 4′,6-diamidino-2-phenylindole (DAPI; #D9542; Sigma Aldrich), and then mounted in Pro Long anti-fade fluorescence medium. Sections were visualized using a LEICA TCS SP5 II confocal laser-scanning microscope (Leica Microsystems, Wetzlar, Germany).

2.7. Western blotting

For the immunoblot experiments, hypothalamus and brown adipose tissue (BAT) were homogenized in approximately 10 volumes of solubilization buffer containing 1% Triton X-100, 100 mM Tris (pH 7.4), 100 mM sodium pyrophosphate, 100 mM sodium fluoride, 10 mM EDTA, 10 mM sodium vanadate, 2 mM PMSF and 0.1 mg/mL aprotinin at 4 °C in a "Polytron PTA 20S Generator" (Brinkmann Instruments mode EN 10/35). The protein concentration of samples was determined by the biuret reagent protein assay. One hundred micrograms of protein per samples was separated by SDS-PAGE and transferred to

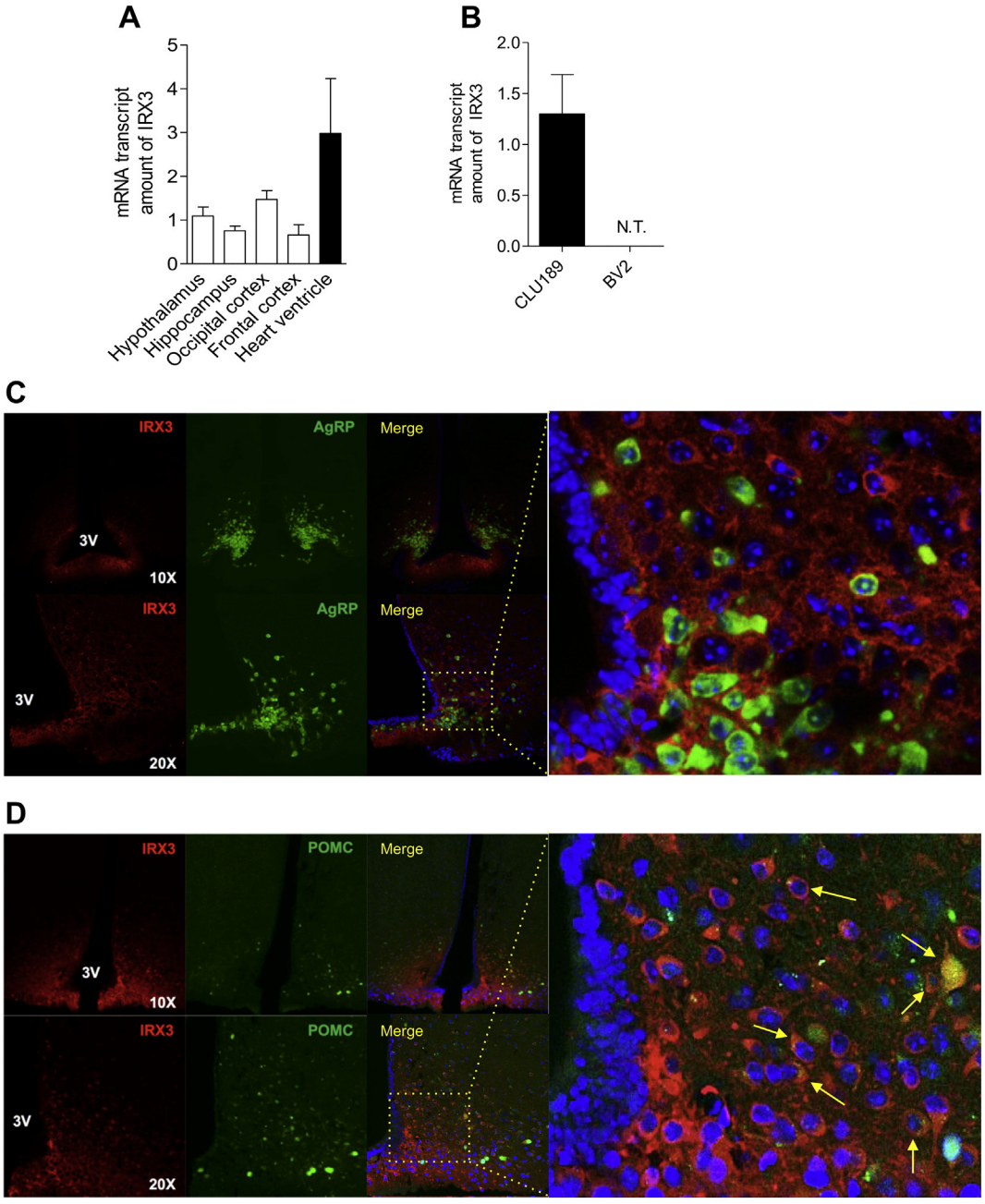

Fig. 1. Irx3/IRX3 expression in mice and cells. The amount of Irx3 transcript in the heart ventricle and brain regions in mice was determined (A), as well as in the hypothalamic neuronal cell-line CLU189 and the microglia cell-line BV2 (B). Immunofluorescence was employed to determine the hypothalamic distribution of IRX3 in AgRP (C) and POMC (D) hrGFP-reporter mice; in D, the yellow arrows indicate co-expression of POMC and IRX3. In A and B, results are expressed as mean ± SEM; n = 5; in C and D, images are representative of three experiments.

nitrocellulose membranes. Blots were blocked in 3% skimmed milk powder solution in TBST (1× TBS and 0.1% Tween 20) for 2 h, washed twice with TBST, and incubated with primary antibodies overnight at 4 °C. The antibodies used are listed in the Supplementary Table 2. HRP-coupled secondary antibodies were used for detection of the conjugate by chemiluminescence, and visualization was achieved by exposure to an Image Quant LAS4000 (GE Healthcare, Life Sciences), using α-tubulin as loading control. Digital quantification of band intensity was performed using Image J software 1.48v (National Health).

2.8. RNA isolation and real-time quantitative polymerase chain reaction (RT-qPCR)

The total RNA content was isolated from homogenized hypothalamus, hippocampus, frontal cortex, and occipital cortex, heart ventricles, BAT or white adipose tissue (WAT) using TRIzol reagent (Invitrogen), according to the manufacturer's recommendations. Two micrograms of total RNA were reverse transcribed to cDNA, according to the manufacturer's instructions (High-Capacity cDNA Reverse Transcription Kit, Life Technologies). Gene expression analyses via real-time quantitative polymerase chain reaction (RT-qPCR) were performed using TaqMan Universal PCR Master Mix (Life Technologies, Carlsbad, CA, USA). RT-qPCR analyses of gene expression were carried out using an ABI Prism 7500 sequence detection system (Applied Biosystems). Primers purchased from Applied Biosystems or Integrated DNA Technologies were used to determine the expression of the endogenous gene *glyceraldehyde 3-phosphate dehydrogenase* (*GAPDH*) in all samples. All other primers (and associated gene IDs) used are listed in Supplementary Table 3. Real-time data were analyzed using the Sequence Detector System 1.7 (Applied Biosystems).

2.9. PCR array

Samples obtained from the hypothalamus of mice 28 days after the bilateral injection of lentiviral vector were used to perform PCR array. Gene expression determination was obtained with RT^2 Profiler™ PCR Array Mouse Inflammatory Cytokines & Receptors (PAMM-011Z, Qiagen), a 96-gene panel that includes 84 genes for inflammatory cytokines/receptors, along with genes for endogenous and positive controls for the PCR reaction (Supplementary Table 4).

2.10. Determination of interscapular brown adipose tissue (iBAT) and tail temperature

In order to determine the interscapular brown adipose tissue (iBAT) and tail thermal release, an infrared camera (IR) was used with an IR resolution of 320 × 240 pixels and a thermal sensitivity and NETD of b40mKat at 30 °C (FLIR T450sc, FLIR Systems, Inc. Wilsonville, USA). Images are presented in the rainbow high-contrast mode that is available in the colour palette of the FLIR Tools software.

2.11. Transmission electronic microscopy (TEM)

For ultrastructural analysis to the brown adipose tissue (BAT), the animals were subjected to transcardiac perfusion with 0.1 M PBS (20 mL, pH 7.4), then fixed with 2.5% glutaraldehyde in cacodilate buffer 0.1 M (pH 7.2) and stored for 2 h at −4 °C. The specimens were post-fixed with osmium in 0.2 M imidazol buffer (pH 7.5), dehydrated and embedded in Durcupan ACS (Fluka, Steinheim, Switzerland). Ultrathin cross sections were collected on formvar coated copper grids, contrasted with uranyl acetate and lead citrate, and examined using a Tecnai G2 Spirit Twin (FEI, Hillsboro, OR) transmission electron microscope operated at 80 kV.

2.12. Single cell RNA sequencing analysis (Drop-seq Analysis)

Bioinformatics analysis of *IRX3* expression was performed using a previously published [12] RNA sequencing library of 20,921 hypothalamic arcuate and median eminence single cells. Heatmaps were generated using the library built-in user interface.

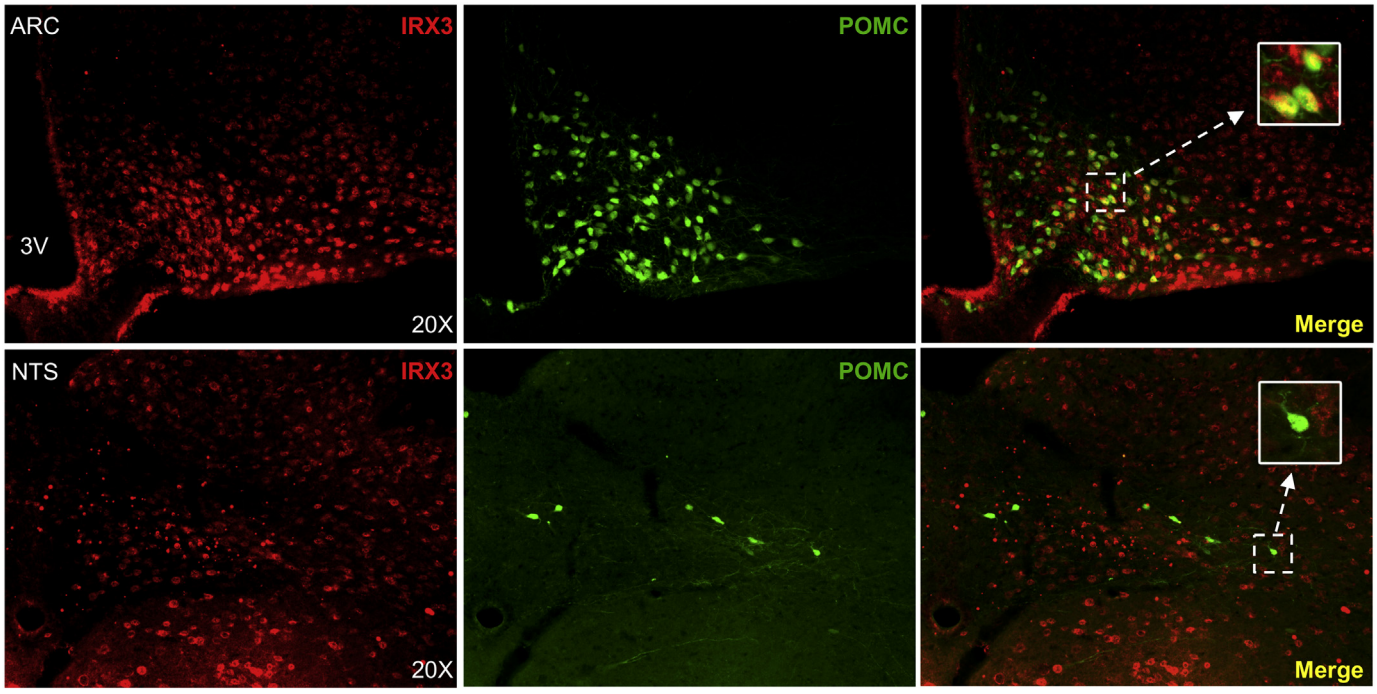

Fig. 2. IRX3 expression in the hypothalamus and solitary tract nucleus of mice. Immunofluorescence was employed to determine the arcuate nucleus (ARC, upper panel) and solitary tract nucleus (NTS, bottom panel) distribution of IRX3 in POMC GFP-reporter mice. In upper panel merge, the inset shows high-magnification image of cells co-expressing POMC and IRX3. In bottom panel merge, the inset shows high-magnification image of a cell that expresses POMC and not IRX3. Images are representative of three experiments.

2.13. Bioinformatics analysis

Correlation analyses were performed with data from hypothalamus tissue samples with distinct phenotypes (BXD Published Phenotypes), employing families of BXD inbred mice as published previously [3]. Row data are accessible on GeneNetwork. Heatmaps were created using GENE-E (The Broad Institute, www.broadinstitute.org/cancer/software/GENE-E/).

2.14. Statistical analysis

All results are reported as the mean ± SEM. Differences between the treatment groups were evaluated using an unpaired Student's *t*-test or a one-way analysis of variance (ANOVA). When the ANOVA indicated significance, a Tukey-Kramer post-hoc test was performed (GraphPad Software, San Diego, CA, USA). A p value <0.05 was considered significant.

3. Results

3.1. Irx3 is expressed in POMC but not AgRP neurons in the hypothalamus

In agreement with a previous study [14], we confirmed that Irx3 is highly expressed in the heart ventricle (Fig. 1A). In the brain, we found considerable amounts of Irx3 transcripts, about half the amount found in the heart, in all regions tested: hypothalamus, hippocampus, and occipital and frontal cortices (Fig. 1A). High expression of Irx3 was also detected in a hypothalamic neuronal cell-line (CLU189), but not in a microglia cell-line (BV2) (Fig. 1B). Using AgRP (Fig. 1C) and POMC (Fig. 1D) hrGFP-reporter mice, large numbers of Irx3 expressing cells were identified in the median eminence and peri-ventricular region of the mediobasal hypothalamus. Co-localization was detected with POMC, but not with AgRP neurons. In another set of experiments, using another POMC GFP reporter mice, the expression of IRX3 was confirmed in hypothalamic POMC cells (Fig. 2, upper panel) but no IRX3 was detected in the POMC subpopulation in the NTS (Fig. 2, bottom panel) [16]. In addition, bioinformatics analysis from a scRNA-seq library of hypothalamic arcuate and median eminence cell types identified high Irx3 expression in a few neurons (Fig. 3A–B). Two of these expressed Pomc (Fig. 3B–C), whereas none expressed Agrp. In most of the high Irx3 expressing cells there was an inverse relation between transcript levels of Irx3 and Fto (Fig. 3A–C); this was particularly true for Pomc neurons that expressed Irx3 (Fig. 3C). The graphic representation of Irx3 expression as determined in the drop-seq analysis in all clusters of cells and in neuron clusters are depicted in Suppl. Figs. 2 and 3, respectively.

3.2. Hypothalamic Irx3 is regulated in response to a high-fat diet

Mice fed a HFD for one or three days (Fig. 4A–B), four weeks (Fig. 4C–D) or eight weeks (Fig. 4E–F) presented with increased body mass and reductions of Npy and Agrp after three days (Fig. 4B);

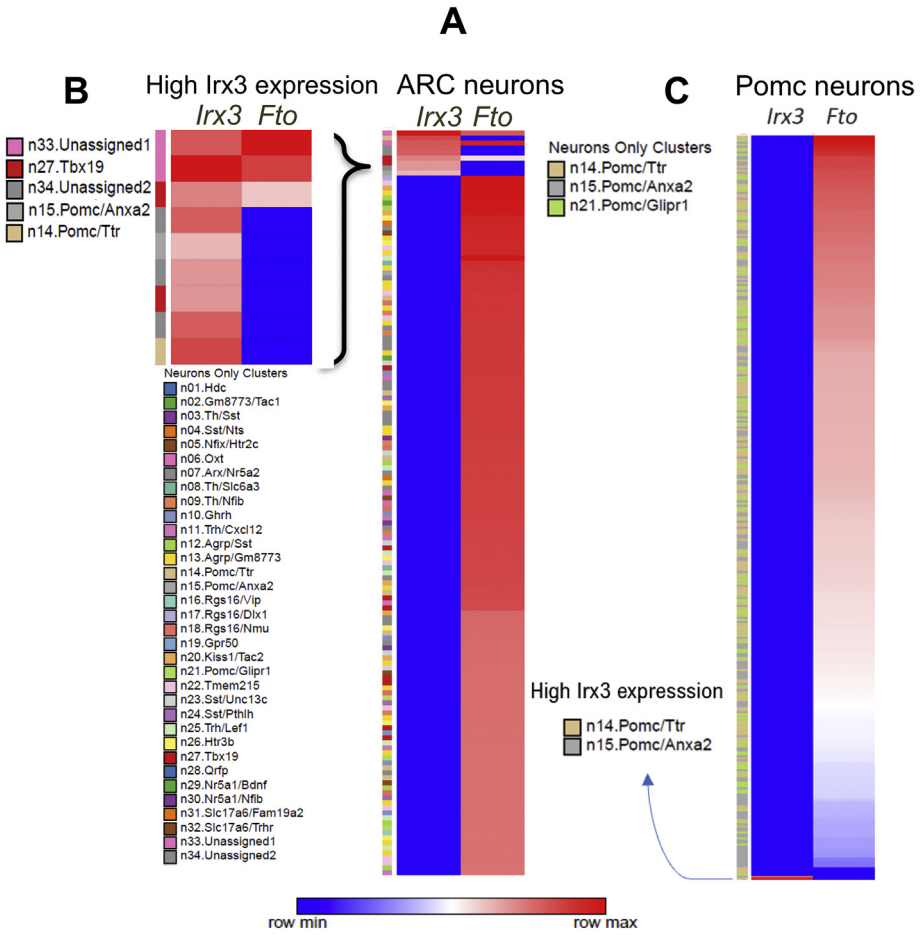

Fig. 3. Irx3 expression in a hypothalamic single-cell RNA sequencing library. The expression of Irx3 was determined by scRNAseq analysis using a library of 20,921 single cells from hypothalamic arcuate nucleus and median eminence from mice, generated by Droplet-Sequencing (A-C). In A, Irx3 and Fto expression in single neurons and clusters. In B, high-magnification view of the neuron clusters expressing highest levels of Irx3. In C, expression of Irx3 and Fto in Pomc single cells. Data production and analysis were performed using the library built-in user interface.

increased POMC after four weeks (Fig. 4D), and reduction of Agrp after eight weeks (Fig. 4F). No significant changes were found in hypothalamic Cart at the time points tested. The hypothalamic expression of Irx3 was reduced after three days, and after four and eight weeks on a HFD (Fig. 4G). This was accompanied by increased expression of hypothalamic Fto four and eight weeks after the introduction of a HFD (Fig. 4H).

3.3. The consumption of a HFD disturbs the physiological pattern of regulation of hypothalamic Irx3

Mice fed standard chow or a HFD for three days were submitted to a protocol to determine the impact of fasting on the expression of hypothalamic Irx3 (Fig. 5A). In mice fed standard chow (Fig. 5B), prolonged fasting (24 h) resulted in the reduction of hypothalamic Irx3,

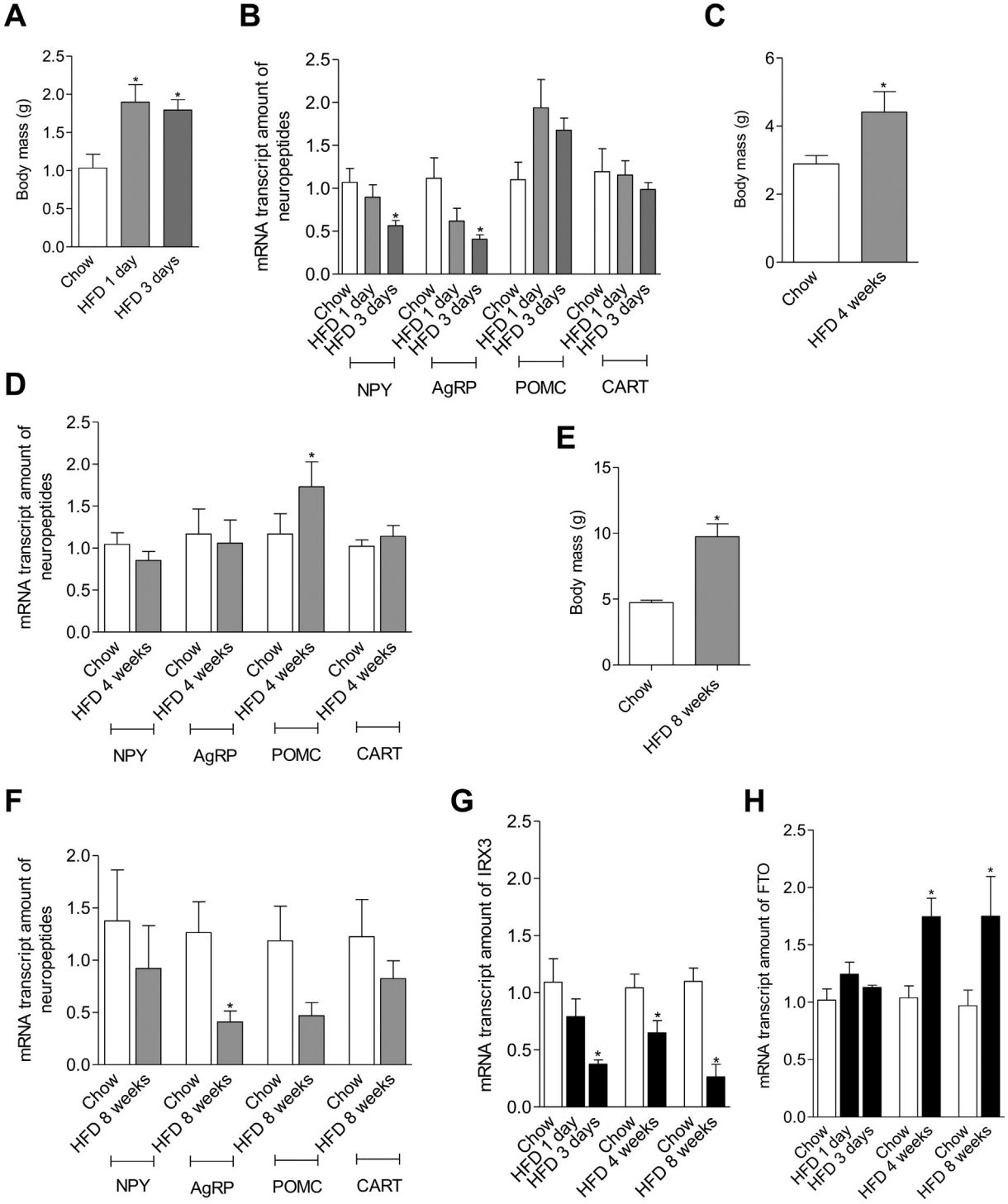

Fig. 4. Modulation of hypothalamic Irx3 by a high-fat diet. Body mass variation of mice fed a high-fat diet (HFD) after one or three days (A), four (C) and eight weeks (E). Neuropeptide analyses of hypothalamus of mice fed HFD at one or three days (B), four (D) and eight weeks (F). Irx3 and Fto transcript expressions (G and H) during the same periods in A-F, in HFD fed mice. In all experiments, except D, n = 5; in D, n = 9. In all experiments *p < 0.05 vs. respective control (chow).

accompanied by increased Npy and Agrp, with no changes in Pomc and Cart. However, when mice were fed a HFD, the physiological regulation pattern of Irx3 and the neurotransmitters were lost (Fig. 5C).

3.4. Inhibition of hypothalamic IRX3 results in body mass gain

We tested five distinct lentiviruses for inhibiting hypothalamic IRX3 (Fig. 6A). Lentivirus 5 (LV5) was the most efficient, resulting in approximately 50% reduction of the IRX3 protein expression (Fig. 6A), and was the only one employed in the remaining experiments. After one day, the hypothalamic inhibition of IRX3 in mice fed a HFD resulted in increased caloric intake (Fig. 6B) and increased body mass (Fig. 6C–D). These parameters were analyzed again at the end of the fourth week of IRX3 inhibition and significantly higher body mass persisted (not shown). There was no change in lean mass (Fig. 6E); however, there was a significant increase in fat mass (Fig. 6F), which was accompanied by an increase in energy storage efficiency (Fig. 6G). Moreover, the inhibition of hypothalamic IRX3, resulted in the abolition of the ability of the HFD to increase O_2 consumption (Fig. 6H) and CO_2 production (Fig. 6I), both in the dark and light phases, respectively. There was also a reduction of respiratory quotient during the light phase in mice fed a HFD (Fig. 6J). Inhibiting hypothalamic IRX3 resulted in increased expression of hypothalamic Fto (Fig. 6L), a trend to increase Npy (Fig. 6M), a significant increase in Agrp (Fig. 6N), no change in Pomc (Fig. 6O), and an increase in Cart in mice fed a HFD, only (Fig. 6P). In addition, the inhibition of IRX3 resulted in an increase in the number of c-Fos positive cells in the paraventricular nucleus, a reduction in the number of c-Fos positive cells in the lateral hypothalamus and no change in c-Fos positive cells in the ventromedial hypothalamus (Suppl. Fig. 4).

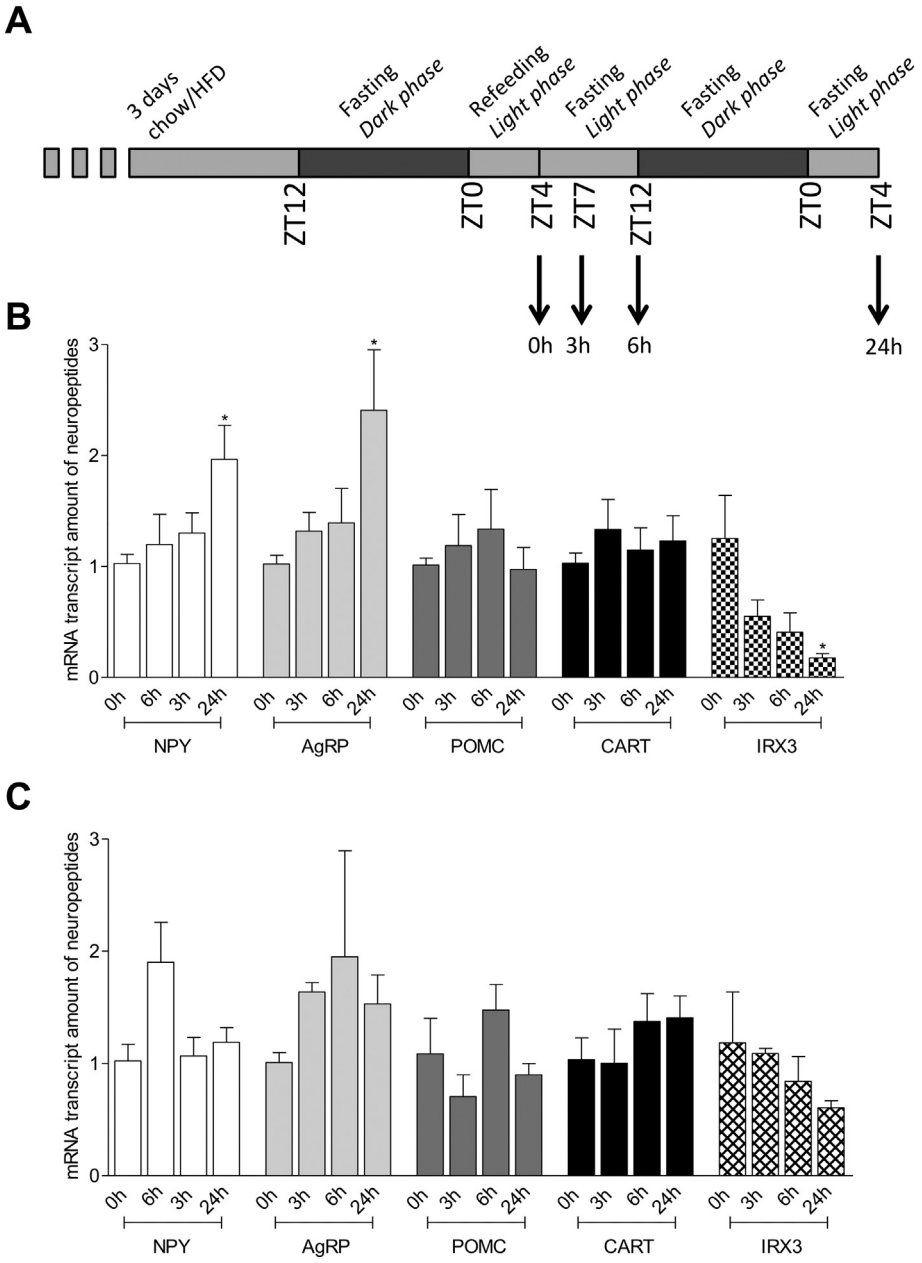

Fig. 5. The effect of fasting on the hypothalamic expression o Irx3 and neuropeptides. Mice were submitted to the fasting protocol as depicted in A; the light/dark cycle and the time of tissue extraction is indicated. Transcript expressions of Npy, Agrp, Pomc, Cart and Irx3 were determined in hypothalamic samples of mice fed chow (B) or a high-fat diet (C). In all experiments, n = 5; *p < 0.05 vs. respective control (0 h fast). ZT0-ZT12, Zeitgeber time 0-12 h.

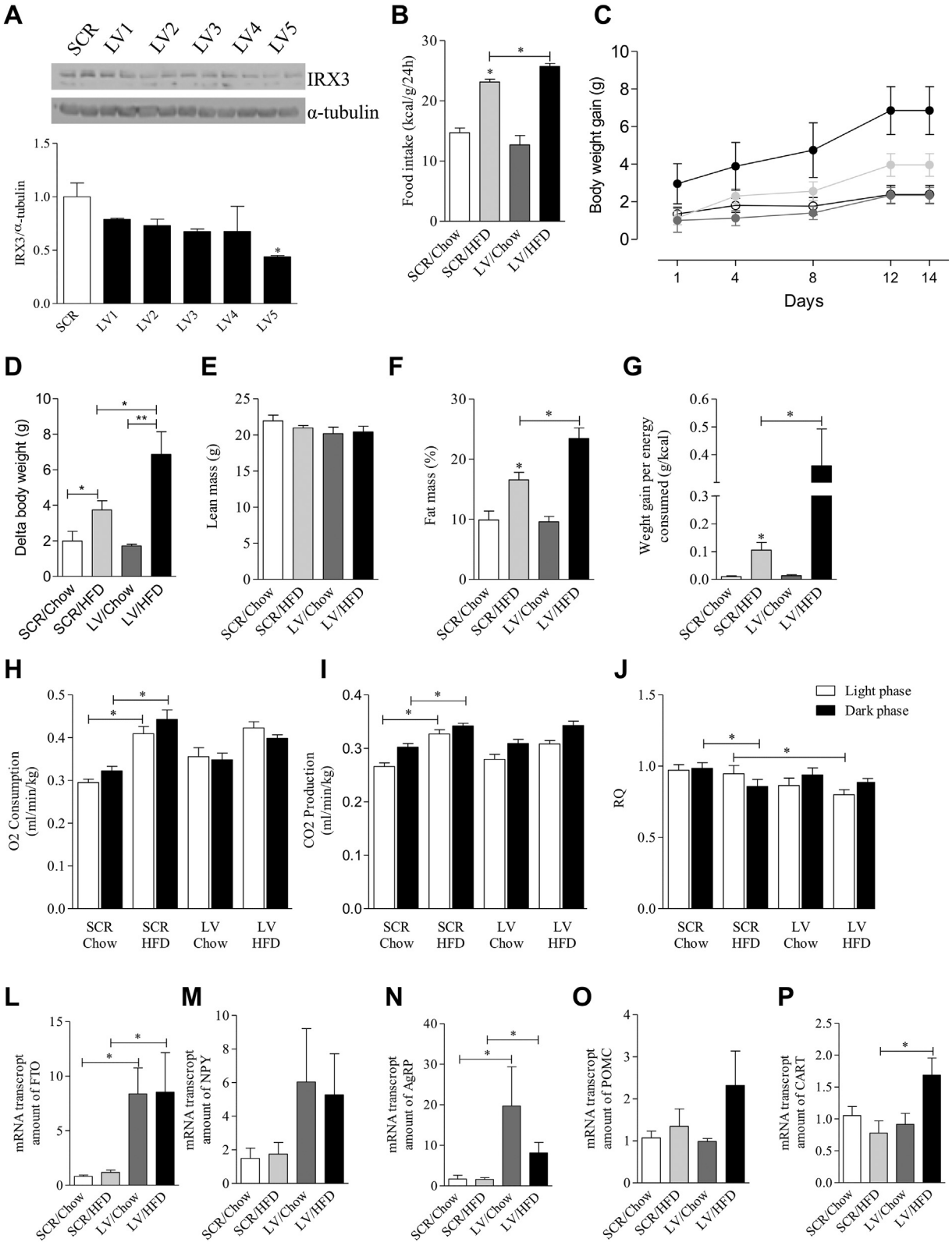

Fig. 6. Phenotype and hypothalamic gene expression in mice with IRX3 inhibition. Five distinct lentiviruses (LV1–LV5) were tested for their efficiency to inhibit the expression of hypothalamic IRX3; the protein level of IRX3 was determined by immunoblot (A). Mice were subjected to a bilateral injection of lentivirus LV5 or a scramble lentivirus (SCR) in the arcuate nucleus, and fed on chow or a high-fat diet (HFD) and the following parameters were evaluated: caloric intake (B), body mass gain (C–D), lean mass (E), fat mass (F), efficiency to store energy (G), O_2 consumption (H), CO_2 production (I), respiratory quotient (RQ) (J), and the hypothalamic transcript expressions of Fto (L), Npy (M), Agrp (N), Pomc (O) and Cart (P). In all experiments, except A and B, parameters were evaluated 28 days after lentivirus injection. In all experiments n = 6; *$p < 0.05$ vs. respective control, or as indicated in the graph.

3.5. The inhibition of hypothalamic IRX3 increases the expression of inflammatory genes in the hypothalamus

Because the inhibition of IRX3 in the hypothalamus resulted in the worsening of the obese phenotype in mice fed a HFD, we asked if increased sign of inflammation in the hypothalamus could accompany this outcome. In a PCR array that evaluated the expression of 84 inflammatory genes we detected a predominant increase in inflammatory genes following the inhibition of IRX3 (Fig. 7A). Significant increases were found in Spp1, Ccr6, Tnfsd11, Ccl8 and Ccl24 expression, whereas significant decreases were found in Il2r and Osm (Fig. 7B). All genes analyzed and the complete name of the genes is presented Supplementary Table 4.

3.6. The inhibition of hypothalamic IRX3 is accompanied by molecular, structural and functional changes in the brown adipose tissue

We hypothesized that part of the effect of hypothalamic IRX3 inhibition on increased body mass gain associated with reduced energy expenditure could be due to impaired brown adipose tissue (BAT) activity. In fact, the inhibition of hypothalamic IRX3 resulted in reduced expression of BAT UCP1 in mice fed a HFD (Fig. 8A and B) and no changes in the expression of BAT PGC1a (Fig. 8A and C) and cytochrome C (Fig. 8A and D). In addition, inhibiting hypothalamic IRX3 resulted in increased BAT beta-3 adrenergic receptor in mice fed standard chow, and a trend towards a reduction in mice fed a HFD (Fig. 8A and E). The total mass of BAT was not affected by the inhibition of hypothalamic IRX3 (Fig. 8F); however, BAT temperature increased in mice fed standard chow and was unaffected in mice fed a HFD (Fig. 8G–H). There were no changes in tail temperature (Suppl. Fig. 5). Transmission electron microscopy revealed that the amount and size of lipid droplets increased in the BAT of mice subjected to hypothalamic IRX3 inhibition (Fig. 8I). The inhibition of hypothalamic IRX3 also affected the expression of browning/beiging genes in white adipose tissue, resulting in the reduction of UCP1 and TBX1 (Fig. 9A); there was also an increase in the white adipose tissue TNFα (Fig. 9B) but no significant changes in lipogenic protein transcripts such as PPARγ, SCD1 and SCD2 (Fig. 9C).

3.7. Bioinformatics analyses support findings on phenotypic effect of IRX3 inhibition

Using a public databank containing genetic and phenotypic features of BXD inbred mice, we sought to determine whether a variation in hypothalamic expression of Irx3 would be accompanied by changes in metabolically related hypothalamic neurotransmitter transcripts and systemic phenotypes related to whole body energy homeostasis. There was a 1.53-fold variation in hypothalamic Irx3 levels among the evaluated mice families (Fig. 10A). Subsequently, a strong positive correlation was seen between hypothalamic Irx3 and Cart or Pomc (Fig. 10B), and no correlation of Irx3 with Npy or Agrp (Fig. 10B). In addition, there was a negative correlation between Irx3 and Fto in the hypothalamus (Fig. 10B). The hypothalamic levels of Irx3 transcripts strongly correlated with the protein levels of UCP1 in BAT (Fig. 10C, upper panel) and with the whole body respiratory exchange ratio (Fig. 10C, bottom panel). Conversely, hypothalamic Irx3 was inversely correlated with body mass gain and adiposity (Fig. 10C, lower panel). Fig. 10D depicts a summary network of the analyzed genes and phenotypes.

4. Discussion

The main objective of this study was to explore the hypothesis that hypothalamic IRX3 could be regulated by the consumption of a high-fat diet, and therefore, that it plays a mechanistic role in the development of diet-induced obesity. This rational was based on the fact that knocking out the *Irx3* gene in mice resulted in a lean phenotype due to increased BAT-dependent energy expenditure [33]; however, little was known about the role of *Irx3* in obesity.

IRX3 was first identified as a member of the *Drosophila Iroquois*-complex, which is a conserved family of homeobox genes present in plants and animals [7,11]. Early studies provided evidence for the role of IRX3 in neural and whole body embryonic development, particularly in antero-posterior patterning and anatomical regionalization of limbs [9,15]. It was also shown that IRX genes are involved in the development of the heart [14], during which IRX3 plays a critical role in the precise regulation of electrical impulse propagation [41]. In 2010, a study showed that IRX3 could be related to type 2 diabetes and obesity [28]; however, it was only in 2014 that the actual nature of this association

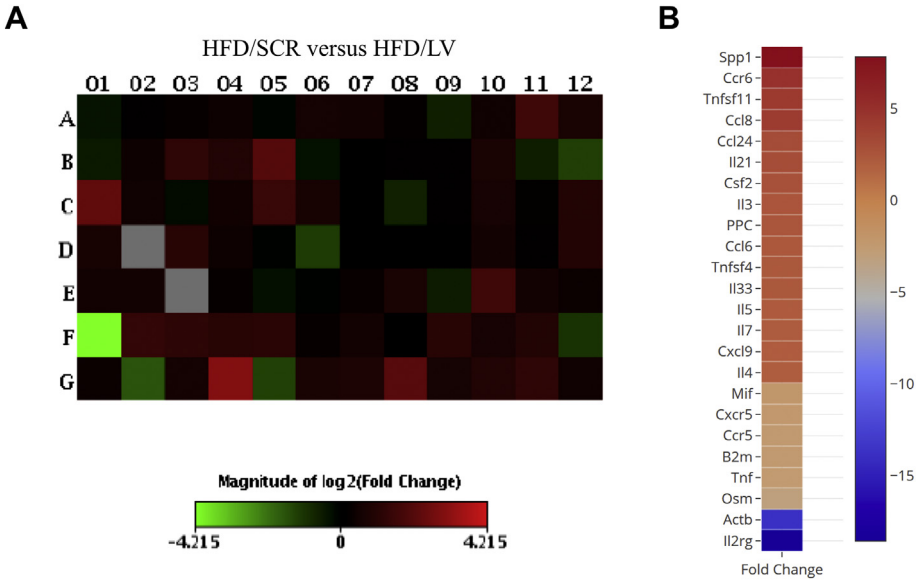

Fig. 7. Expression of transcripts encoding inflammatory proteins in the hypothalamus of mice with inhibited IRX3. Heat map illustrating the results of a PCR array for inflammatory genes (A). Genes with the highest and lowest expression change in the hypothalamus of IRX3-inhibited mice fed a high-fat diet (HFD), compared to mice treated with a scramble lentivirus (LV) (SCR) (B). Results are representative of three independent experiments. Ccl8, chemokine (C-C motif) ligand 8; Ccl24, chemokine (C-C motif) ligand24; Ccr6, chemokine receptor 6; Il2r, interleukin 2 receptor; Osm, oncostatin M; Spp1, secreted phosphoprotein 1; Tnfsf11, tumor necrosis factor superfamily member 11.

was defined [33]. Both whole-body knockout (KO) mice and those with hypothalamic-specific dominant negative *Irx3* developed lean body phenotypes due to increased energy expenditure and activation of the BAT thermogenic gene signature [33], suggesting that hypothalamic IRX3 is involved in the sympathetic control of BAT function. Still, to date little is known about the putative regulation of hypothalamic IRX3 by dietary factors and obesity.

Developmental studies have shown that *Irx3* is involved in the early organization of the hypothalamus [13,25], and that the deletion of the chromosome region that harbors the *Irx3* gene, such as the one found in the fused toes mouse mutant, leads to severe hypothalamic malformation [4]. However, no previous study has explored the anatomical and cellular distribution of IRX3 in the hypothalamus. First, the present study confirms high expression of Irx3 in the heart as previously demonstrated [28]. In addition, its expression was also high in distinct

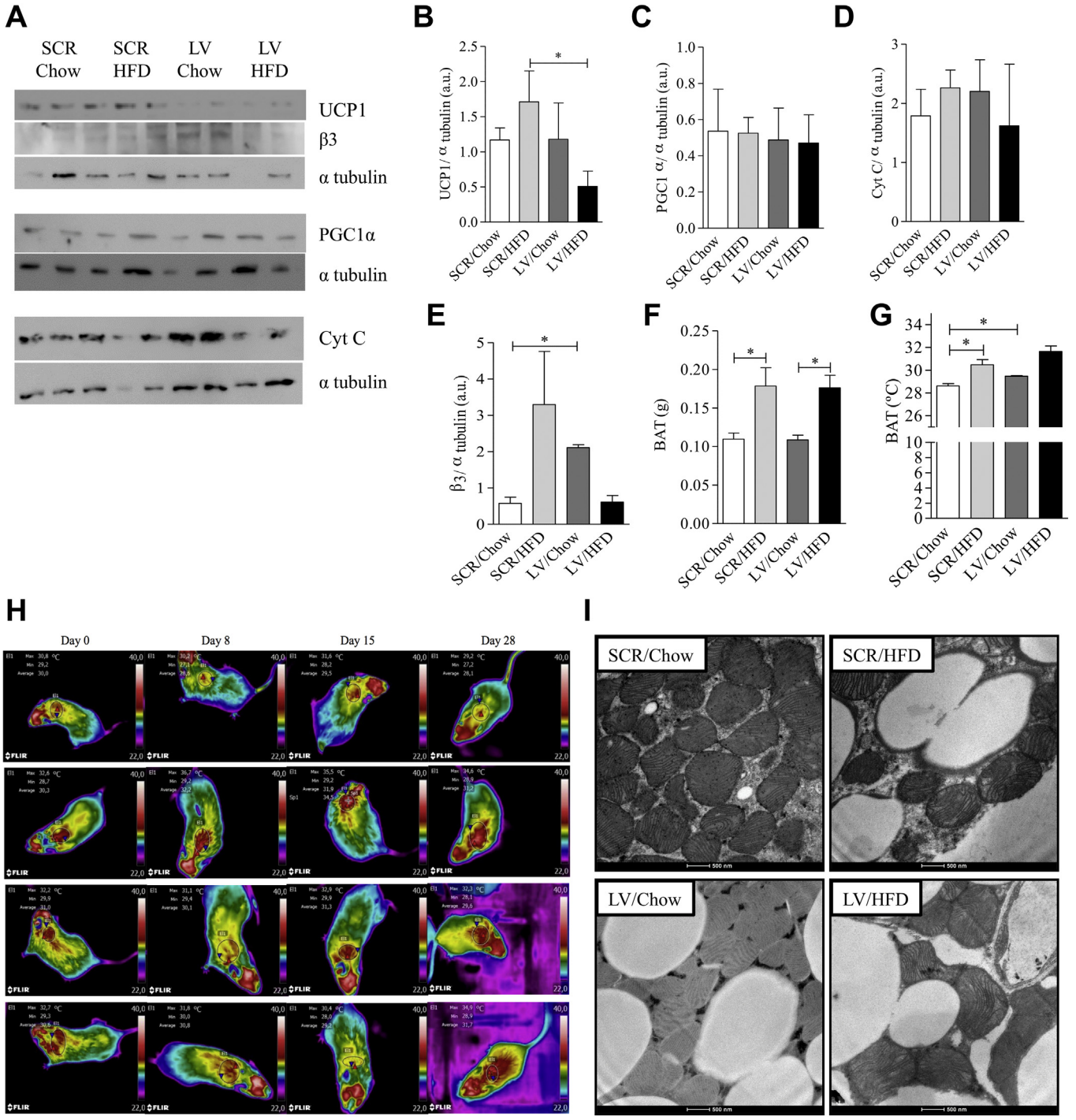

Fig. 8. Brown adipose tissue changes in mice with an inhibition of hypothalamic IRX3. Mice were subjected to a bilateral injection of lentivirus LV5 (LV) or a scramble lentivirus (SCR) in the arcuate nucleus, and fed on chow or a high-fat diet (HFD); after 28 days parameters were evaluated. The expression of uncoupling protein 1 (UCP1) (A and B), peroxisome proliferator-activated receptor gamma coactivator 1-alpha (PGC1α) (A and C), cytochrome C (Cyt C) (A and D) and beta 3 adrenergic receptor (β3) (A and E) in the brown adipose tissue were determined by immunoblot, employing α-tubulin as housekeeping protein. Brown adipose tissue mass was determined (F), as well as interscapular temperature (G and H). Fragments of the brown adipose tissue were harvested and prepared for transmission electron microscopy (I). In A–E, n = 6, *p < 0.05; in F-H, n = 8; *p < 0.05; in I, images are representative of three independent experiments.

areas of the brain, including the hypothalamus. In this particular region, the expression seemed to occur predominantly in POMC neurons; both in immunofluorescence experiments using POMC and AgRP reporter mice, and in a drop-seq experiment that evaluated >20,000 hypothalamic neurons, IRX3 was only found in POMC neurons [12]. We also performed an additional set of experiments in order to evaluate if IRX3 could be also present in the lorcaserin-sensitive NTS POMC neurons [16]. Using a different strategy to obtain POMC reporter mice, we confirmed the expression of IRX3 in hypothalamic but not in NTS POMC neurons. Studies have shown that proper function of POMC neurons is essential for body mass stability [2]. In a timely study [10], researchers generated a reversible genetic model of early-onset hyperphagia and obesity in rodents by selectively blocking the expression of the *Pomc* gene in hypothalamic neurons. By doing so, the authors demonstrated that the longer POMC expression was absent, the more difficult it was to reestablish normal body mass after the reactivation of gene expression. Furthermore, it has been shown that POMC expression is affected very early after the introduction of a HFD, and that distinct patterns of POMC regulation of in mice exposed to a HFD can predict the obese-resistant or the obese-propensity phenotypes [34]. Thus, should IRX3 impact the regulation of POMC, it could play an important role in whole body energy homeostasis and metabolism.

To explore the potential regulation of IRX3 by dietary factors, mice were exposed to prolonged fasting and to a HFD. It was clear that hypothalamic IRX3 regulation changes in response to fasting and feeding in such way that the longer the fasting period, the lower the Irx3 expression. When mice were fed a HFD, the physiological pattern of hypothalamic Irx3 regulation was lost, suggesting that the consumption of dietary fats could have a direct impact on Irx3 expression. In fact, the HFD alone was capable of reducing hypothalamic expression of Irx3 significantly after three days, an outcome that persisted for at least eight weeks. This is the first evidence that consumption of dietary fats can disturb hypothalamic Irx3 expression.

It was previously shown that whole body KO of *Irx3* or the expression of a dominant negative *Irx3* in the hypothalamus resulted in leanness and activation of BAT [33]. The majority of the experiments performed in that study employed mice fed standard chow [33]. To gain further insight into the potential involvement of hypothalamic Irx3 in diet-induced obesity, we inhibited Irx3 in the hypothalamus using a lentivirus and fed mice a HFD. To our surprise, dissimilar to the results reported by Smemo et al. [33], the inhibition of hypothalamic Irx3 resulted in increased gain in body mass due to increased adiposity. Under hypothalamic Irx3 inhibition mice consumed more calories and presented with attenuation of HFD-induced increase of whole body O_2 consumption/CO_2 production, suggesting a reduction of energy expenditure. This was further supported by an increase in weight gain per calorie consumed, suggesting that hypothalamic inhibition of Irx3 in obese mice resulted in improved storage efficiency of whole body energy. Furthermore, the inhibition of hypothalamic Irx3 resulted in a reduction of UCP1 expression in BAT and a trend towards a reduction of the beta-3 adrenergic receptor, which was accompanied by increased BAT adiposity. Interestingly, only minor phenotypic changes occurred when hypothalamic Irx3 was inhibited in mice fed standard chow.

The mechanism behind the changes in whole body energy homeostasis seen in this mouse model may be related to the effect of hypothalamic IRX3 on the expression of Agrp and Fto; both genes significantly increase when IRX3 is inhibited. The role of FTO in the control of energy homeostasis and body mass is still controversial. Studies have shown that FTO RNA demethylase activity is linked to the regulation of adipogenesis [40], dopamine circuitry in the midbrain [22] and the activation of ghrelin to control the response to food cues [24]. However, it seems that this control occurs in a dose dependent way [24], which may explain why studies have not been able to provide evidence of any correlation between hypothalamic FTO expression and the magnitude of obesity. Regarding AgRP, there is a more straightforward correlation between hypothalamic expression and body adiposity [1,21]. AgRP has an important role in the regulation of both food intake and energy expenditure [1,21]. However, considering IRX3 is present mostly in POMC neurons, why does its inhibition affect AgRP expression while having only a minor effect on POMC? POMC neurons are known to be rapidly and transiently regulated in response to fasting and feeding [34]; thus, it could be argued that, despite the fact that we did not detect significant changes in POMC, at certain points during the fasting-feeding cycle it could be changed to promote a regulation of AgRP, as previously shown [19,36]. Further studies are required to evaluate the short-term effects of IRX3 regulation on POMC expression.

Lastly, bioinformatics were employed to determine if different hypothalamic transcript levels of Irx3 correlated with Fto and neurotransmitters in the hypothalamus, and also with some phenotypic parameters related to whole body energy expenditure. A similar approach was

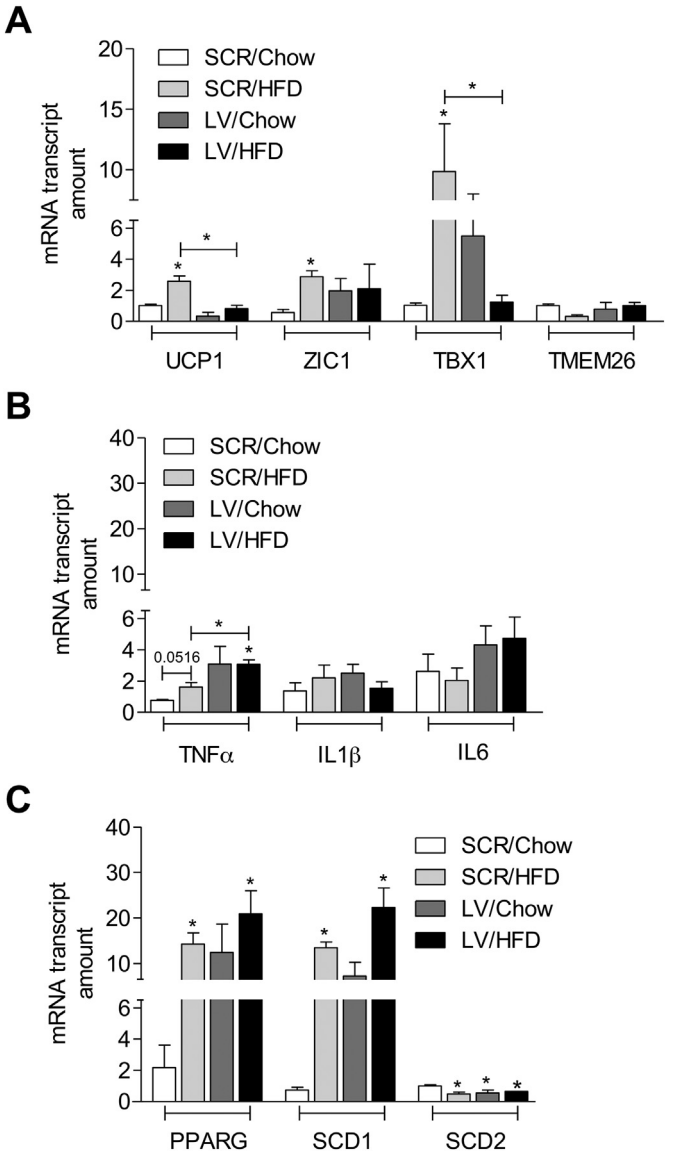

Fig. 9. White adipose tissue changes in mice with an inhibition of hypothalamic IRX3. Mice were subjected to a bilateral injection of lentivirus LV5 (LV) or a scramble lentivirus (SCR) in the arcuate nucleus, and fed on chow or a high-fat diet (HFD); after 28 days parameters were evaluated in the white adipose tissue. Real-time PCR was employed to determine transcript expressions of the browning/beiging markers, uncoupling protein 1 (UCP1), zinc finger protein of the cerebellum 1 (ZIC1), T-box protein 1 (TBX1) and transmembrane protein 26 (TMEM26) (A); the inflammatory cytokines, tumor necrosis factor-alpha (TNFα), interleukin 1-beta (IL1β) and interleukin 6 (IL6) (B); and the lipogenic proteins, peroxisome proliferator-activated receptor gamma (PPARG), stearoyl Co-A desaturase 1 (SCD1), and stearoyl Co-A desaturase 2 (SCD2) (C). In all experiments $n = 6$; *$p < 0.05$ vs. respective control or as demonstrated in the panel.

used to characterize metabolic traits establishing a reliable systems genetics method to study the correlation of transcript expression with both genetic and phenotypic features [3]. There was 1.53-fold variation in the hypothalamic levels of Irx3 transcript among the mouse families that were evaluated in this study. This variation positively correlated with Pomc, yet negatively correlated with Fto. Most importantly, hypothalamic Irx3 positively correlated with BAT UCP1 and respiratory exchange ratio, and negatively correlated with body mass gain and adiposity, which is in agreement with our experimental findings using the lentivirus to inhibit hypothalamic IRX3.

This is only the second study evaluating the potential involvement of hypothalamic IRX3 in whole body energy homeostasis. Surprisingly, the phenotype obtained when we inhibited hypothalamic IRX3 was opposite to the one obtained in the study by Smemo et al. [33]. There are two differences that could explain the divergent phenotypes: first, both models employed by Smemo et al. [33] had any IRX3 expression at all, whereas in our model, IRX3 was reduced by 50%; second, both models employed by Smemo et al. [33] had a lack of IRX3 beginning at the embryonic life stage, whereas we inhibited IRX3 during adulthood. This could be an issue because studies have shown that IRX3 is important for a number of aspects of neuronal development, including the appropriate development of the hypothalamus [13,25]; thus, extended structural and cellular evaluation of the hypothalamus of the mutants could provide information to help gain an understanding of the differences between phenotypes. Concerning the differences in the amount of hypothalamic IRX3 protein, it has been argued that IRX3 protein levels operate in a hormetic fashion [8] to control hypothalamic function. In fact, in our bioinformatics analysis, despite the negative correlation between hypothalamic Irx3 and body mass gain, in the two families with the highest hypothalamic Irx3 expression, body mass gain increased, supporting a hormetic regulation of Irx3 actions. Studies using transgenes to express different levels of IRX3 in the hypothalamus could help solve this question.

In conclusion, hypothalamic IRX3 is modulated by fasting/feeding cycles, and diet-induced obesity disturbs this cycle, keeping IRX3 levels lower than the baseline. Further reduction of hypothalamic IRX3 in obesity models intensifies the obese phenotype due to a higher caloric intake and reduced energy expenditure. This work provides additional evidence for the important role played by hypothalamic IRX3 in the control of whole body homeostasis.

Author contributions

TMA performed most experiments, designed experiments under supervision of LAV and YBK; prepared figures under supervision of LAV, wrote paper under supervision of LAV; DSR and FCS helped TMA in immunofluorescence and PCR experiments; JCLJ helped TMA in brown adipose tissue functional experiments; RSG and DSO performed bioinformatics analysis; SCV performed transmission electron microscopy experiments; JDJ performed some of the POMC reporter mice

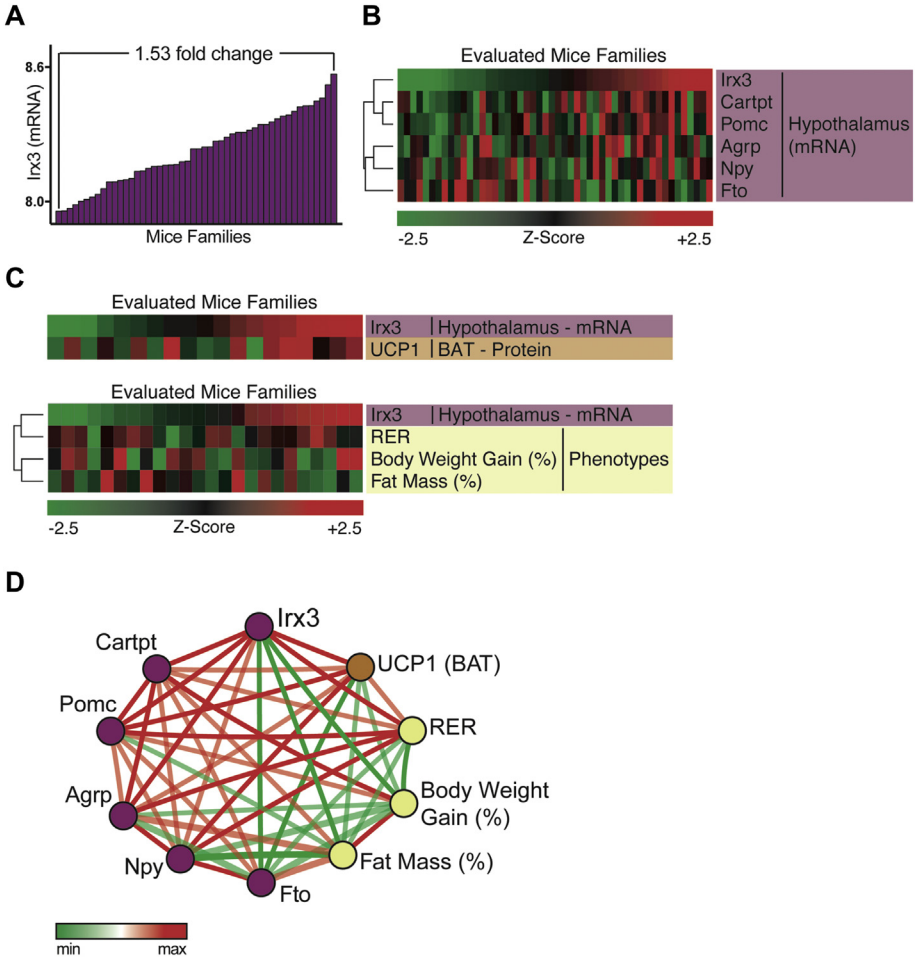

Fig. 10. Bioinformatics analysis of hypothalamic Irx3 in mouse reference families. Hypothalamic variation in Irx3 transcript expression among the families of isogenic BXD mice (A). Heatmap depicting the hypothalamic levels of Irx3 in comparison with neurotransmitters and Fto (B). Heatmap of the correlations between hypothalamic Irx3 and brown adipose tissue (BAT) UCP1 protein (C, upper panel) or the phenotypes of respiratory exchange ratio (RER), body mass gain and fat mass (C, lower panel). Summary network of the hypothalamic transcripts evaluated in this analysis (D); green connectors define negative correlation and red connectors define positive correlation; n = 14–50 BXD mouse families.

experiments; YBK supervised TMA fellowship in Boston during the time he performed some of the experiments with POMC reporter mice and analysis of droplet-sequencing, YBK also provided important insights in the experimental design and in the writing of the manuscript; LAV is supervisor for TMA, planned the study, designed experiments, prepared manuscript and obtained most grants.

Acknowledgements

We thank Erika Roman, Gerson Ferraz, Marcio Cruz and Joseane Morari from the University of Campinas for technical assistance. The Laboratory of Cell Signaling belongs to the Obesity and Comorbidities Research Center and the National Institute of Science and Technology – Neuroimmunomodulation. Sao Paulo Research Foundation grants 2013/07607-8 (LAV) and 2017/02983-2 (JDJ); NIH grants R01DK083567 (YBK).

Competing financial interests

The authors have no financial interests to declare.

Appendix A. Supplementary data

Supplementary data to this article can be found online at https://doi.org/10.1016/j.ebiom.2018.11.048.

References

[1] Al-Qassab H, Smith MA, Irvine EE, Guillermet-Guibert J, Claret M, Choudhury AI, et al. Dominant role of the p110beta isoform of PI3K over p110alpha in energy homeostasis regulation by POMC and AgRP neurons. Cell Metab 2009;10:343–54.
[2] Andermann ML, Lowell BB. Toward a wiring diagram understanding of appetite control. Neuron 2017;95:757–78.
[3] Andreux PA, Williams EG, Koutnikova H, Houtkooper RH, Champy MF, Henry H, et al. Systems genetics of metabolism: the use of the BXD murine reference panel for multiscalar integration of traits. Cell 2012;150:1287–99.
[4] Anselme I, Laclef C, Lanaud M, Ruther U, Schneider-Maunoury S. Defects in brain patterning and head morphogenesis in the mouse mutant Fused toes. Dev Biol 2007;304:208–20.
[5] Araujo EP, Moraes JC, Cintra DE, Velloso LA. Mechanisms in endocrinology: hypothalamic inflammation and nutrition. Eur J Endocrinol 2016;175:R97-105.
[6] Arruda AP, Milanski M, Coope A, Torsoni AS, Ropelle E, Carvalho DP, et al. Low-grade hypothalamic inflammation leads to defective thermogenesis, insulin resistance, and impaired insulin secretion. Endocrinology 2011;152:1314–26.
[7] Bellefroid EJ, Kobbe A, Gruss P, Pieler T, Gurdon JB, Papalopulu N. Xiro3 encodes a Xenopus homolog of the Drosophila Iroquois genes and functions in neural specification. EMBO J 1998;17:191–203.
[8] Bhakta-Guha D, Efferth T. Hormesis: decoding two sides of the same coin. Pharmaceuticals (Basel) 2015;8:865–83.
[9] Bosse A, Zulch A, Becker MB, Torres M, Gomez-Skarmeta JL, Modolell J, et al. Identification of the vertebrate Iroquois homeobox gene family with overlapping expression during early development of the nervous system. Mech Dev 1997;69:169–81.
[10] Bumaschny VF, Yamashita M, Casas-Cordero R, Otero-Corchon V, de Souza FS, Rubinstein M, et al. Obesity-programmed mice are rescued by early genetic intervention. J Clin Invest 2012;122:4203–12.
[11] Burglin TR. Analysis of TALE superclass homeobox genes (MEIS, PBC, KNOX, Iroquois, TGIF) reveals a novel domain conserved between plants and animals. Nucleic Acids Res 1997;25:4173–80.
[12] Campbell JN, Macosko EZ, Fenselau H, Pers TH, Lyubetskaya A, Tenen D, et al. A molecular census of arcuate hypothalamus and median eminence cell types. Nat Neurosci 2017;20:484–96.
[13] Caqueret A, Boucher F, Michaud JL. Laminar organization of the early developing anterior hypothalamus. Dev Biol 2006;298:95–106.
[14] Christoffels VM, Keijser AG, Houweling AC, Clout DE, Moorman AF. Patterning the embryonic heart: identification of five mouse Iroquois homeobox genes in the developing heart. Dev Biol 2000;224:263–74.
[15] Cohen DR, Cheng CW, Cheng SH, Hui CC. Expression of two novel mouse Iroquois homeobox genes during neurogenesis. Mech Dev 2000;91:317–21.
[16] D'Agostino G, Lyons D, Cristiano C, Lettieri M, Olarte-Sanchez C, Burke LK, et al. Nucleus of the solitary tract serotonin 5-HT2C receptors modulate food intake. Cell Metab 2018;28:619–30 [e615].
[17] De Souza CT, Araujo EP, Bordin S, Ashimine R, Zollner RL, Boschero AC, et al. Consumption of a fat-rich diet activates a proinflammatory response and induces insulin resistance in the hypothalamus. Endocrinology 2005;146:4192–9.
[18] Dina C, Meyre D, Gallina S, Durand E, Korner A, Jacobson P, et al. Variation in FTO contributes to childhood obesity and severe adult obesity. Nat Genet 2007;39:724–6.
[19] Elias CF, Aschkenasi C, Lee C, Kelly J, Ahima RS, Bjorbaek C, et al. Leptin differentially regulates NPY and POMC neurons projecting to the lateral hypothalamic area. Neuron 1999;23:775–86.
[20] Frayling TM, Timpson NJ, Weedon MN, Zeggini E, Freathy RM, Lindgren CM, et al. A common variant in the FTO gene is associated with body mass index and predisposes to childhood and adult obesity. Science 2007;316:889–94.
[21] Gropp E, Shanabrough M, Borok E, Xu AW, Janoschek R, Buch T, et al. Agouti-related peptide-expressing neurons are mandatory for feeding. Nat Neurosci 2005;8:1289–91.
[22] Hess ME, Hess S, Meyer KD, Verhagen LA, Koch L, Bronneke HS, et al. The fat mass and obesity associated gene (Fto) regulates activity of the dopaminergic midbrain circuitry. Nat Neurosci 2013;16:1042–8.
[23] Ignacio-Souza LM, Bombassaro B, Pascoal LB, Portovedo MA, Razolli DS, Coope A, et al. Defective regulation of the ubiquitin/proteasome system in the hypothalamus of obese male mice. Endocrinology 2014;155:2831–44.
[24] Karra E, O'Daly OG, Choudhury AI, Yousseif A, Millership S, Neary MT, et al. A link between FTO, ghrelin, and impaired brain food-cue responsivity. J Clin Invest 2013;123:3539–51.
[25] Kobayashi D, Kobayashi M, Matsumoto K, Ogura T, Nakafuku M, Shimamura K. Early subdivisions in the neural plate define distinct competence for inductive signals. Development 2002;129:83–93.
[26] Milanski M, Degasperi G, Coope A, Morari J, Denis R, Cintra DE, et al. Saturated fatty acids produce an inflammatory response predominantly through the activation of TLR4 signaling in hypothalamus: implications for the pathogenesis of obesity. J Neurosci 2009;29:359–70.
[27] Moraes JC, Coope A, Morari J, Cintra DE, Roman EA, Pauli JR, et al. High-fat diet induces apoptosis of hypothalamic neurons. PLoS One 2009;4:e5045.
[28] Ragvin A, Moro E, Fredman D, Navratilova P, Drivenes O, Engstrom PG, et al. Long-range gene regulation links genomic type 2 diabetes and obesity risk regions to HHEX, SOX4, and IRX3. Proc Natl Acad Sci U S A 2010;107:775–80.
[29] Rossi MA, Stuber GD. Overlapping brain circuits for homeostatic and hedonic feeding. Cell Metab 2018;27:42–56.
[30] Schneeberger M, Dietrich MO, Sebastian D, Imbernon M, Castano C, Garcia A, et al. Mitofusin 2 in POMC neurons connects ER stress with leptin resistance and energy imbalance. Cell 2013;155:172–87.
[31] Scuteri A, Sanna S, Chen WM, Uda M, Albai G, Strait J, et al. Genome-wide association scan shows genetic variants in the FTO gene are associated with obesity-related traits. PLoS Genet 2007;3:e115.
[32] Seoane-Collazo P, Martinez De Morentin PB, Ferno J, Dieguez C, Nogueiras R, Lopez M. Nicotine improves obesity and hepatic steatosis and ER stress in diet-induced obese male rats. Endocrinology 2014;155:1679–89.
[33] Smemo S, Tena JJ, Kim KH, Gamazon ER, Sakabe NJ, Gomez-Marin C, et al. Obesity-associated variants within FTO form long-range functional connections with IRX3. Nature 2014;507:371–5.
[34] Souza GF, Solon C, Nascimento LF, De-Lima-Junior JC, Nogueira G, Moura R, et al. Defective regulation of POMC precedes hypothalamic inflammation in diet-induced obesity. Sci Rep 2016;6:29290.
[35] Thaler JP, Yi CX, Schur EA, Guyenet SJ, Hwang BH, Dietrich MO, et al. Obesity is associated with hypothalamic injury in rodents and humans. J Clin Invest 2012;122:153–62.
[36] Toda C, Santoro A, Kim JD, Diano S. POMC neurons: from birth to death. Annu Rev Physiol 2017;79:209–36.
[37] Tung YCL, Yeo GSH, O'Rahilly S, Coll AP. Obesity and FTO: changing focus at a complex locus. Cell Metab 2014;20:710–8.
[38] van de Sande-Lee S, Pereira FR, Cintra DE, Fernandes PT, Cardoso AR, Garlipp CR, et al. Partial reversibility of hypothalamic dysfunction and changes in brain activity after body mass reduction in obese subjects. Diabetes 2011;60:1699–704.
[39] Velloso LA, Schwartz MW. Altered hypothalamic function in diet-induced obesity. Int J Obes (Lond) 2011;35:1455–65.
[40] Zhang M, Zhang Y, Ma J, Guo F, Cao Q, Zhang Y, et al. The demethylase activity of FTO (Fat Mass and Obesity Associated Protein) is required for preadipocyte differentiation. PLoS One 2015;10:e0133788.
[41] Zhang SS, Kim KH, Rosen A, Smyth JW, Sakuma R, Delgado-Olguin P, et al. Iroquois homeobox gene 3 establishes fast conduction in the cardiac His-Purkinje network. Proc Natl Acad Sci U S A 2011;108:13576–81.
[42] Zhang X, Zhang G, Zhang H, Karin M, Bai H, Cai D. Hypothalamic IKKbeta/NF-kappaB and ER stress link overnutrition to energy imbalance and obesity. Cell 2008;135:61–73.